# Solution properties of poly(vinylidene fluoride): 2. Relation between microgel formation and microstructure

**G. Lutringer*, B. Meurer and G. Weill**
*Institut Charles Sadron (CRM-EAHP), Université L. Pasteur, 6 rue Boussingault, 67083 Strasbourg Cedex, France*
*(Received 7 November 1989; revised 22 February 1990; accepted 6 April 1990)*

In contrast to type I poly(vinylidene fluoride) (PVDF), solutions of type II PVDF contain, even in good solvents, a fraction of microgel that cannot be fully eliminated for characterization by light scattering. Intrinsic viscosity and size exclusion chromatography reveal that the soluble fraction has a molecular mass in the same range as type I samples, which are fully soluble in the same solvents. The shear moduli in the molten state reveal that the microgel fraction does not contain a high enough molecular mass to explain microgel formation by phase separation. From an analysis of the $^{19}F$ nuclear magnetic resonance spectra of both suspension- and emulsion-polymerized PVDF samples, with first-order Markov statistics, microgel formation is attributed to differences in microstructure, involving sequences with two reversed additions in a row.

**(Keywords: poly(vinylidene fluoride); microgel; size exclusion chromatography; $^{19}F$ nuclear magnetic resonance; microstructure)**

## INTRODUCTION

We have reported in part 1[1] that poly(vinylidene fluoride) (PVDF) can be readily soluble in many solvents with an interaction parameter $\chi$ going from $\sim 0.5$ (dimethylsulphoxide (DMSO), dimethylformamide (DMF)) to negative values (*N*,*N*'-dimethyl-*N*,*N*'-trimethylene urea (DMPU)). This PVDF was referred to as type I PVDF. In contrast, other PVDF samples (referred to as type II PVDF) cannot be totally dissolved in all these solvents and always present a microgel fraction. We present in this part 2 a study of the origin of this microgel. We first try to eliminate the microgel and to characterize the soluble fraction by light scattering (LS), intrinsic viscosity and size exclusion chromatography (s.e.c.). We then evaluate whether the microgel fraction can contain very high molecular masses from rheological measurements in the molten state. From swelling experiments we obtain a value for the mean distance between crosslinks in the microgel. We then carry out a $^{19}F$ n.m.r. study of the microstructure of types I and II PVDF and calculate from the parameters of the first-order Markov process for the polymerization kinetics some possible sequences responsible for the formation of microgels.

## SAMPLES AND EXPERIMENTAL PROCEDURES

Type II PVDF samples were commercial products from Pennwalt Co., USA (Kynar 460) and Atochem, France (Foraflon 50, 1000, 2500 and 9000). Laboratory-polymerized type II PVDF samples (denoted B1 to B5) with a larger variation in microstructure were also provided by Atochem. Totally soluble samples (of type I) used for the n.m.r. study are described in part 1[1].

Light-scattering (LS) experiments have been carried out on the supernatant liquid from centrifuged solutions. A gel fraction always remains in the bottom of the centrifugation tube. Its volume and concentration was measured to get information on the percentage of material participating in the microgel and its degree of swelling. In all experiments, particularly when heating has been used to try to improve dissolution, a check for fluorescence resulting from polyene sequences formed by dehydrofluorination has been carried out by visual inspection (when using a mercury lamp) or by measurement of the polarization of the scattered light (when using a He–Ne laser). Intrinsic viscosities have been measured on solutions of samples first reprecipitated in water to eliminate residual surfactant and diminish polyelectrolyte effects[2]. There is no qualitative difference in gel formation between raw and washed material.

Size exclusion chromatography (s.e.c.) has been carried out with a set of three Microstyragel columns (porosity $10^3$, $10^4$ and $10^5$ Å) in DMF. Microgel appears as the first peak, which can be suppressed by use of a first 'filtering' column (porosity $10^6$ Å). The amount of microgel can be evaluated from the area of the chromatogram of the soluble fraction. Shodex columns have been used with *N*-methylpyrrolidone (NMP)/0.1 M LiBr salt (see part 1[1]). In this latter case, multiple detection with either light scattering (LS) or viscosity ($[\eta]$) has been made available to us in Atochem's laboratory in a selected number of cases.

Shear modulus measurements in the molten state have been carried out on a Rheometrics instrument in either the dynamic ($G^*(\omega)$) or the relaxation ($G(t)$) mode. $G(t)$ has been transformed to $G^*(\omega)$ in the very low-frequency range according to Schwarzl[3].

$^{19}F$ N.m.r. spectra have been recorded on a Bruker AM 400 spectrometer. Most experiments have been

* Present address: Ciba-Geigy, Basel, Switzerland

0032-3861/91/050884-08

carried out in mixtures of DMAc and either DMF-$d_7$ or acetone-$d_6$, at concentrations of ~7–8% (w/v). To ensure a quantitative evaluation of different band areas, the averaging has been carried out with repetition rates adapted to the measured $T_1$ values (0.6–0.9 s) and the spectral width has been limited to 50 kHz, allowing the use of a 16-bit converter. In the search for extra lines, a spectral width of 75 kHz (≃200 ppm) has been used, limiting the dynamics to that of a 12-bit converter (1/2000). Chemical shifts are given with respect to $CFCl_3$. $^{19}F$ spectra are $^1H$-decoupled. It has been checked that Overhauser enhancement is uniform.

## MACROMOLECULAR CHARACTERIZATION

### *Light scattering*

All efforts to eliminate the presence of microgel by increasing the solvent quality, increasing the dissolution temperature in the range 80–120°C or decreasing the polymer concentration have failed. After centrifugation, the Zimm plot of the supernatant liquid remains in all cases characteristic of the presence of dense particles of high molecular mass as evidenced by:

(i) an upward curvature in the angular dependence $P^{-1}(\theta)$ (*Figure 1*);

(ii) a weight-average molecular mass of several millions.

Typical values of $M_w$ for a type II PVDF in a series of solvents (*Table 1*) seem consistent, but the values of the mean-square radius of gyration $\langle s^2\rangle_z$ and second virial coefficient $A_2$ are much smaller than extrapolated from our results on fully soluble samples[1], as expected for aggregates. Similarly, experiments carried out on a series of type II PVDF in DMAc show some consistency between the apparent molecular masses and the melt index (*Table 2*) but the apparent $\langle s^2\rangle_z$ varies roughly with the power 2/3 of the apparent $M_w$ (*Figure 2*), again in favour of aggregates making the major contribution to the scattering.

### *Intrinsic viscosities*

Dense aggregates should very weakly contribute to the intrinsic viscosity, which should thus give a reliable molecular mass of the soluble fraction, using the Mark–Houwink relations obtained for soluble polymers in part 1[1] after correction for the polymer concentration, calculated from the fraction $f$ of microgel.

In the first experiments carried out in DMAc we have found a polyelectrolyte effect[2] due to some remaining ionic surfactant of emulsion-polymerized PVDF. It can be eliminated by water reprecipitation, washing with a water–ethanol mixture followed by vacuum drying. It does not, however, suppress the presence of aggregates.

*Table 3* gives the values of the apparent intrinsic viscosity $[\eta]_{app}$ and Huggins constant $k$, the corrected value $[\eta]_{corr} = [\eta]_{app}(1-f)^{-1}$ and the molecular mass calculated using the Mark–Houwink relation obtained in part 1. These molecular masses are one order of magnitude smaller than measured by light scattering and for the Foraflon series respect the order of the melt index.

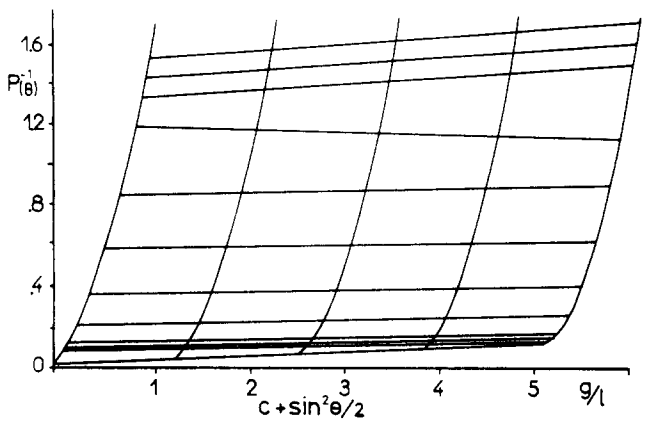


**Figure 1** Zimm plot measured on type II PVDF in DMAc. One obtains $M_w = 9.9 \times 10^6$ g mol$^{-1}$, $A_2 = 2.9 \times 10^{-5}$ cm$^3$ g$^{-2}$ mol and $\langle s^2\rangle_z^{1/2} = 217$ nm

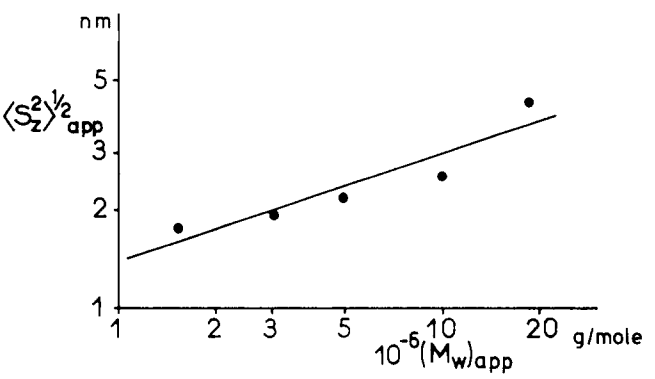


**Figure 2** Root-mean-square radius of gyration $\langle s^2\rangle_z^{1/2}$ *versus* apparent molecular mass as measured by light scattering. A straight line of slope 1/3 fits the data well

**Table 1** Light-scattering data with microgel present as a function of solvent quality (sample F1000)

| Solvent | DMSO | DMF | DMAc | NMP | DMPU | HMPT |
|---|---|---|---|---|---|---|
| $M_w \times 10^{-3}$ (g mol$^{-1}$) | 9000 | 4000 | 5000 | 5000 | 5000 | 5000 |
| $\langle s^2\rangle_z^{1/2}$ (nm) | 280 | 200 | 220 | 230 | 230 | 200 |
| $A_2 \times 10^5$ (cm$^3$ g$^{-2}$ mol) | −5 | −0.5 | 0.3 | 0.7 | 0.9 | 1 |

**Table 2** Light-scattering data for a series of polymers with microgel in DMAc

| Sample | F9000 | F2500 | F1000 | F50 | K460 |
|---|---|---|---|---|---|
| $M_w \times 10^{-3}$ (g mol$^{-1}$) | 1500 | 3000 | 5000 | 9900 | 19 000 |
| $\langle s^2\rangle_z^{1/2}$ (nm) | 180 | 195 | 220 | 250 | 450 |
| Melt index (g/10 min) | 82–90 | 14–22 | 7–13 | <7 | |

**Table 3** Intrinsic viscosities (dl $g^{-1}$), Huggins constant and calculated molecular mass in DMAc

| Sample | F9000 | F2500 | F1000 | F50 | K460 |
|---|---|---|---|---|---|
| $[\eta]_{app}$ | 1.03 | 1.19 | 1.26 | 1.625 | 0.98 |
| $k$ | 0.33 | 0.37 | 0.42 | 0.47 | 0.57 |
| $[\eta]_{corr}$ | 1.08 | 1.24 | 1.32 | 1.74 | $\simeq 2$ |
| $M_w \times 10^{-3}$ (g $mol^{-1}$) | 146 | 177 | 194 | 295 | 345 |

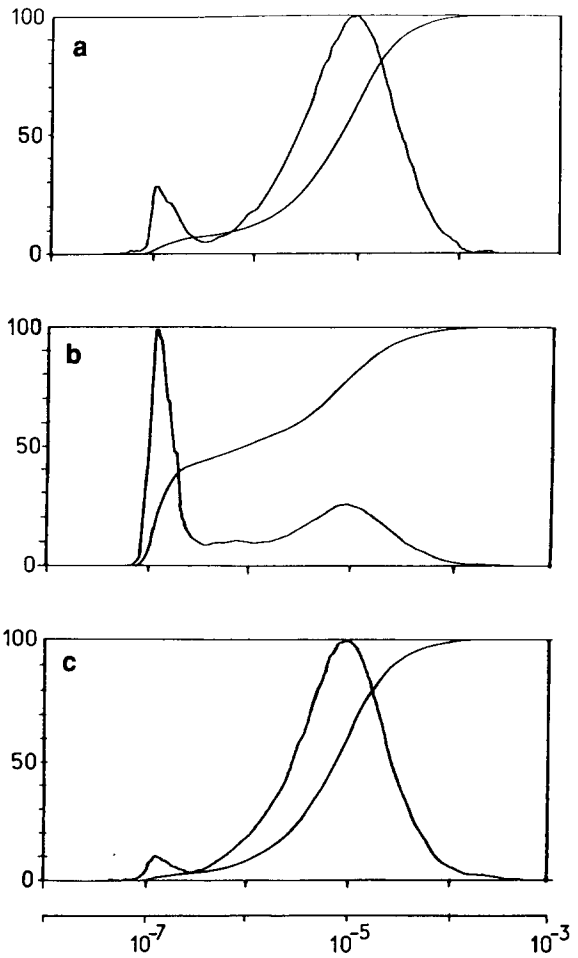


**Figure 3** S.e.c. chromatograms of a type II PVDF in DMF (concentration *versus* volume of elution). The bottom scale gives the correspondence between volume of elution and molecular weight. Traces: (a) after washing, (b) gel fraction, (c) supernatant

*Size exclusion chromatography*

A typical chromatogram of a type II PVDF in DMF at 90°C without a filtering column is shown in *Figure 3* for a solution, its supernatant and its gel fraction. The presence of microgel in the supernatant liquid is confirmed: the swollen gel also contains, as expected, a fraction of soluble molecules. The fraction of microgel $f$ can be calculated from the relative area of the two peaks. The apparent molecular mass $M_w$ and polymolecularity index $I_p$ of the soluble fraction have been calculated from the second peak using poly(ethylene oxide) (PEO) or polystyrene (PS) calibration:

$$f = 8\% \qquad M_{w,PEO} = 203 \times 10^3 \qquad I_p = 2.7$$
$$M_{w,PS} = 408 \times 10^3 \qquad I_p = 2.5$$

From the relation between apparent and true molecular masses found in part 1, the true $M_w$ is of order $200 \times 10^3$, in fair agreement with the viscosity behaviour of this sample.

**Table 4** Size exclusion chromatography data in NMP/LiBr at 85°C

| Sample | Gel fraction, $f$ (%) | $I_p$ | $M_w \times 10^{-3}$ (g $mol^{-1}$) PS | Corrected | $[\eta]_{coupl}$ | $LS_{coupl}$ |
|---|---|---|---|---|---|---|
| F9000 | 3.5 | 2.5 | 199 | 170 | | |
| F6000 | 5.5 | 2.4 | 209 | 180 | | |
| F4000 | 5.1 | 2.5 | 226 | 195 | | |
| F2500 | 6.5 | 2.5 | 255 | 215 | | |
| F1000 | 7.6 | 2.5 | 288 | 245 | 185 | 234 |
| F50 | 13 | 2.5 | 396 | 330 | | 400 |
| K460 | 44 | 4.0 | 367 | 307 | 398 | 420 |
| B1 | 35 | 5.1 | 175 | 150 | | |
| B2 | 17 | 3.8 | 111 | 98 | | |
| B3 | 17 | 2.8 | 415 | 345 | | |
| B4 | $\simeq 0$ | 3.0 | 356 | 300 | | |
| B5 | 22 | 4.8 | 358 | 300 | | |

A complete survey of the samples has been carried out by s.e.c. in NMP/LiBr at 85°C. With Shodex columns the microgel is filtered out and its fraction $f$ is calculated from a quantitative evaluation of the area of the refractometric signal. Only PS calibration has been used and a 'true $M_w$' has been deduced from $M_{w,PS}$ using the relation established in part 1[1]:

$$M_w = 1.4 M_{w,PS}^{0.96}$$

Results are reported in *Table 4*. In a few cases where a light-scattering detector or a viscosimetric detector has been made available to us, the results of LS/refractometric or $[\eta]$/refractometric coupling using the universal calibration are also given in *Table 4*.

Considering all the approximations the results are fairly consistent and in good agreement with those from intrinsic viscosity.

No direct correlation appears between the fraction of microgel and the molecular mass of the soluble fraction.

*Rheological studies*

In order to eliminate the possibility that microgel formation results from the demixing of a fraction of much higher molecular mass, we have carried out a rheological study of the whole microgel and supernatant fractions of Foraflon 1000 and Kynar 460 in order to obtain their zero-frequency viscosity, which is known to scale as $M^{3.4}$.

For that purpose the imaginary part of the dynamic viscosity $\eta'(\omega) = G''(\omega)/\omega$ has been plotted as a function of the real part $\eta''(\omega) = G'(\omega)/\omega$ (Cole–Cole procedure) (*Figure 4*). The fit by an arc with its centre below the real axis reveals a non-exponential relaxation or a distribution of relaxation times, also found in $G(t)$. The fact that the angle made by the line joining the centre of the circle to the origin with the real axis is independent

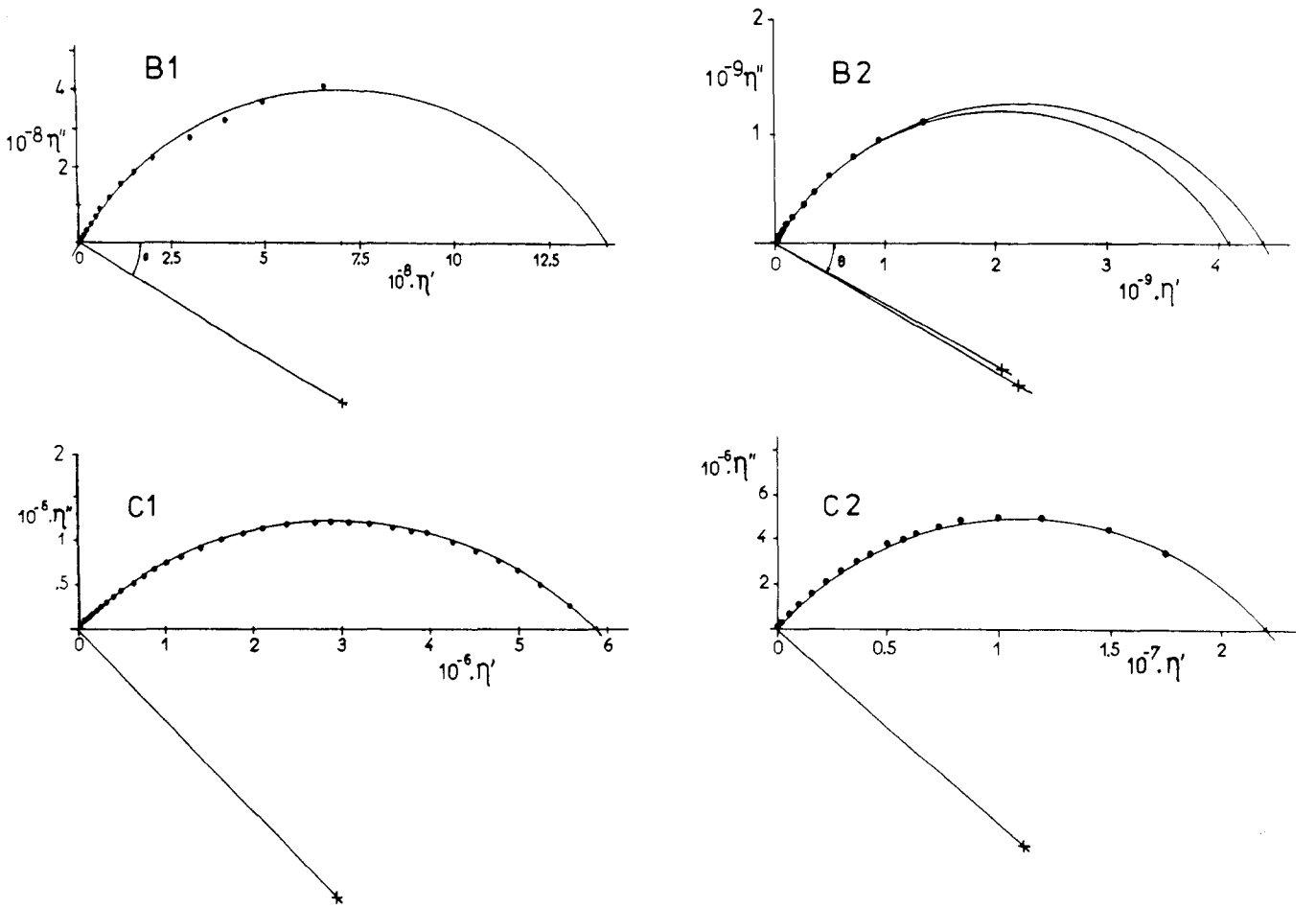


**Figure 4** Master curve Cole–Cole plots of dynamic viscosity (experiments at temperatures between 220 and 300°C shifted to 220°C, viscosity in poises). Plots: (B1) gel fraction of Foraflon 1000; (C1) supernatant of Foraflon 1000; (B2) gel fraction of Kynar 460; (C2) supernatant of Kynar 460

of temperature indicates that the time–temperature superposition principle holds. However, at these temperatures well above $T_g$, the WLF relation can hardly be distinguished from an Arrhenius relation for the shift factor. An apparent activation energy of $147 \pm 8$ kJ mol$^{-1}$ has been found. Zero-frequency viscosities (*Figure 4*) for the supernatant $\eta_S$ and the gel $\eta_G$ are typically in the ratio of $\sim 200$, indicating a ratio of molecular weights of $\sim 5$ for the two kinds of PVDF. Such a value completely rules out the possibility that microgel formation, observed even in very good solvents of soluble samples (see part 1[1]), results from phase separation of a fraction of ultrahigh molecular mass. Such a hypothesis is in fact also borne out by the high swelling observed in the centrifuged gel fraction.

*Swelling of the gel in DMAc*

The degree of swelling has been calculated from the volume of the gel separated by centrifugation of a 3.5% solution and its polymer content obtained by water reprecipitation, vacuum drying and weighing. The swelling ratio $Q$ is then calculated using the value 0.552 cm$^3$ g$^{-1}$ for the specific volume $v_2$ of PVDF.

An evaluation of the mean molecular mass between crosslinks $M_c$ can then be carried out using Flory's theory of equilibrium swelling[4]:

$$Q^{5/3} = v_2 M_c (1 - 2M_c/M)^{-1}(\tfrac{1}{2} - \chi)/V_1$$

where $M$ is the molecular mass of the chains participating in the network, $V_1$ the molar volume of the solvent (92.68 cm$^3$ for DMAc) and $\chi$ the interaction parameter for PVDF in DMAc ($\chi = 0.25$[1]). With these values:

$$Q^{5/3} = 2.47 \times 10^{-3} M_c (1 - 2M_c/M)^{-1} \quad (1)$$

Taking for $M$ either $M_w$ of the soluble fraction or $5M_w$ to take into account the higher molecular mass of the chains in the microgel, found from rheological data, limits for $M_c$ deduced from observed $Q$ by plotting relation (1) are given in *Table 5*. A value of $M_c$ between $35 \times 10^3$ and $220 \times 10^3$, i.e. 500 to 3000 monomeric units, suggests that a few specific sequences, with a probability of the order of $10^{-3}$, tend to associate. Thus the formation of gel will depend on both the molecular mass and the microstructure of the different samples. The possible differences of microstructure among soluble and insoluble samples of PVDF are studied in the next section using high-resolution $^{19}$F n.m.r.

## $^{19}$F NUCLEAR MAGNETIC RESONANCE STUDY

PVDF is one of the polymers where 'head-to-head' (also called backwards or reverse) addition has a non-negligible probability. Owing to the high sensitivity of $^{19}$F chemical shift, high-resolution n.m.r. can detect individual signals arising from different sequences of up to 11 carbons[5–12]. Since many of these signals have relative intensities of the order of $10^{-3}$, their assignment can carry some ambiguities, especially when other defects such as branching or dehydrofluoration or additives

**Table 5** Evaluation of the number of crosslinks per chain from the gel swelling ratio $Q$ ($M_c/M$ gives an idea of the number of crosslinks per chain)

| Sample | $M_w \times 10^{-3}$ in supernatant (g mol$^{-1}$) | $I_p$ | Gel fraction, $f$ (%) | $Q$ | $10^{-3} \times M_c$ (g mol$^{-1}$) | $M_c/M$ |
|---|---|---|---|---|---|---|
| B2 | 100 | 3.8 | 17 | 26 | 35–65 | 3–7 |
| B1 | 150 | 5.1 | 35 | 20 | 40–55 | 3.5–13 |
| F1000 | 240 | 2.5 | 8 | 59 | 100–220 | 2.4–5.5 |
| F50 | 330 | 2.5 | 13 | 53 | 100–200 | 3.3–8 |
| B3 | 340 | 2.8 | 17 | 50 | 100–200 | 3.4–8 |
| K460 | 460 | 4.0 | 44 | 35 | 100–130 | 4.6–17 |

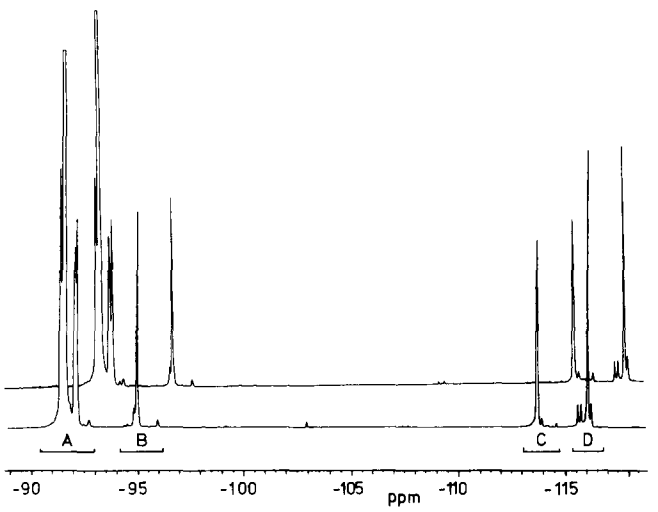


**Figure 5** $^{19}$F n.m.r. spectra at 376 MHz of typical soluble (bottom, Solef 1010) and 'gel-forming' (top, Foraflon 1000) samples: 8% solutions (w/v) in 50/50 (v/v) mixture of DMAc and acetone-$d_6$; $10^4$ scans are averaged for precise evaluation of small lines

interfere[6,11]. Small chemical shift differences in different solvents make comparisons between published data sometimes difficult[5–7]. The assignments of the pentads are, however, completely unambiguous[10] and *Figure 5* shows the four well resolved peaks of two samples representative of soluble and microgel-forming PVDF. A first-order Markov process has been found sufficient for the interpretation of the probability of sequences of up to 11 carbons[6,7]. In what follows we shall derive the parameters of the Markov process from an analysis at the pentad level and calculate when needed the probability of longer sequences using these parameters. Only a few remarks will be made on the comparison of these probabilities with the intensities of the weaker signals, which do not all fit with previous attributions.

*Markov process and n.m.r. intensities*

With a first-order Markov model, the propagation of the PVDF chain is characterized by four rate constants, $k_{FF}$, $k_{FR}$, $k_{RF}$ and $k_{RR}$, corresponding to the four modes of addition (forward F and reverse R):

(a) $\sim CH_2—CF_2^{\bullet} + CH_2=CF_2 \xrightarrow{k_{FF}} \sim CH_2—CF_2—CH_2—CF_2^{\bullet}$

(b) $\sim CH_2—CF_2^{\bullet} + CH_2=CF_2 \xrightarrow{k_{FR}} \sim CH_2—CF_2—CF_2—CH_2^{\bullet}$

(c) $\sim CF_2—CH_2^{\bullet} + CH_2=CF_2 \xrightarrow{k_{RF}} \sim CF_2—CH_2—CH_2—CF_2^{\bullet}$

(d) $\sim CF_2—CH_2^{\bullet} + CH_2=CF_2 \xrightarrow{k_{RR}} \sim CF_2—CH_2—CF_2—CH_2^{\bullet}$

Here (a) is the most probable addition with a probability $p(FF) \simeq 1$; and (b) corresponds to a reversal repaired by addition (c) with a probability $p(RF)$ or propagated by addition (d) with a much lower probability $p(RR)$.

The microstructure of the chain is completely controlled by the two parameters[8]:

$$r_0 = k_{RR}/k_{RF} \qquad r_1 = k_{FF}/k_{FR}$$

since the probabilities of addition can be written for example:

$$p(FF) = k_{FF}[\sim F][M]/\{k_{FR}[\sim F][M] + k_{FF}[\sim F][M]\}$$

$$= \frac{r_1}{1 + r_1} = 1 - x$$

and similarly

$$p(FR) = \frac{1}{1 + r_1} = x$$

$$p(RF) = \frac{1}{1 + r_0} = y$$

$$p(RR) = \frac{r_0}{1 + r_0} = 1 - y$$

Since the probabilities for a forward or reversed growing end $p(F)$ and $p(R)$ are given by:

$$p(F) = p(F)p(FF) + p(R)p(RF)$$

$$p(R) = p(F)p(FR) + p(R)p(RR)$$

one has

$$p(F) = y/(x + y) \qquad p(R) = x/(x + y) = 1 - p(F)$$

If $x$ and $y$ are known, the probability of any sequence can be calculated as a product of known quantities. In order to establish the correspondence between the sequence of monomers and the sequence of $-CH_2-$ and $-CF_2-$ groups, which control $^1$H and $^{19}$F chemical shifts, we follow Cais *et al.*'s notation[8], denoting $CH_2 = 0$ and $CF_2 = 2$. As an example, for a sequence of three monomers FRF, we have

$$p(FRF) = p(F)p(FR)p(RF) = p(022002)$$

Owing to the small range of chemical shift, $^1$H n.m.r.

is limited to the distinction between 2$\underline{0}$2 (no reversal) and 0$\underline{0}$2 (reversed) triads, even at the highest fields available. High-field $^{19}F$ n.m.r. allows easy detection of the four $CF_2$-centred pentads 20$\underline{2}$02, 00$\underline{2}$02, 02$\underline{2}$02 and 02$\underline{2}$00. Assignments of individual lines inside of the well resolved groups may allow a direct detection of sequences of up to 11 carbons[6,7]. The difficulties of assignment due in particular to other defects have been mentioned before and will be the object of another paper[12]. We concentrate here on the pentad assignments and work out the relation between the probabilities of triads and pentads on the one hand (odd number of carbons) and pairs or triplets of monomers on the other (even number of carbons).

At the triad level, one has:

$$p(2\underline{0}2) = \tfrac{1}{2}p(0202) + \tfrac{1}{2}p(2020)$$
$$= \tfrac{1}{2}p(F)p(FF) + \tfrac{1}{2}p(R)p(RR)$$
$$= \tfrac{1}{2} - xy/(x+y)$$
$$p(0\underline{0}2) + p(2\underline{0}0) = p(2002) = p(R)p(RF) = xy/(x+y)$$
$$p(0\underline{2}0) = \tfrac{1}{2}p(0202) + \tfrac{1}{2}p(2020)$$
$$= p(2\underline{0}2) = \tfrac{1}{2} - xy/(x+y)$$
$$p(2\underline{2}0) + p(0\underline{2}2) = p(0220) = p(F)p(FR) = xy/(x+y)$$

$^1H$ and $^{19}F$ give evidently the same results. The use of the two sets of experimental data allows a cross-check. They are insufficient to obtain values of $x$ and $y$, or of $x+y=\alpha$ and $xy=\beta$.

One has to go one step further with $^{19}F$ n.m.r. where, using the same reasoning, one establishes easily:

$p(20\underline{2}02) = \tfrac{1}{2} - 2\beta/\alpha + \beta/2$
group A of lines: $-90$ to $-93$ ppm

$p(00\underline{2}02) = \beta/\alpha - \beta/2$
group B of lines: $-94$ to $-97$ ppm

$p(02\underline{2}02) = \beta/\alpha - \beta/2$
group C of lines: $-113$ to $-115$ ppm

$p(02\underline{2}00) = \beta/2$
group D of lines: $-115$ to $-116$ ppm

The attribution to groups has first been given on the basis of additivity rules[9] for a sequence of seven carbons centred on $CF_2$ (refs. 7 and 9):

$$\delta_i = \delta_7 + \sum a_i$$

where $\delta_7$ is the shift position of the perfluorinated sequence and the $a_i$ are increments for the replacement of one or two $CH_2$ in $\alpha$, $\beta$ and $\gamma$ positions. This is confirmed by the consistency of the values of $\alpha$ and $\beta$ Markov parameters[6,7] and directly by two-dimensional COSY spectra[10].

*Application to a series of soluble and microgel-forming PVDF*

*Table 6* gives the values of the integrated intensities of the A, B, C and D groups of lines. Within experimental error, one has $D > B$ and $B = C$, a signature for a first-order Markov process. Kynar 460 presents an exception with $B > C$ and $C \simeq D$. We have calculated the percentage of reversed monomers and the probabilities of addition for this model from combination of D and A + B (*Table 6*).

Two differences appear clearly between 'soluble' (type I) and 'gel-forming' (type II) samples:

(i) all type II samples have a content of reversed units greater than 5%, while type I samples have mostly $3.8 \leqslant p(R) \leqslant 5.1\%$;

(ii) all type II samples have a high $p(RR)$ compared to type I samples.

Knowing from the swelling experiment that gel formation should be related to the presence of a few ($\simeq 10^{-3}$) specific sequences, it would indeed be difficult to explain large differences in solubility from the small differences in $p(R)$ only. The difference in $p(RR)$ suggests a maximum difference of probability in the two kinds of samples for a sequence of two consecutive reversals: this sequence (0202202002) is of probability

$$p(F)p(FF)p(FR)p(RR)p(RF) \simeq p(FR)p(RR)$$

This product is in the range $(0.4\text{–}4) \times 10^{-4}$ for the

**Table 6** 6 N.m.r. intensities of groups A, B, C and D of lines and computed Markov parameters

| Sample | Gel fraction, $f$ (%) | A | B | C | D | A + B + C + D | $p(R) \times 10^2$ | $p(FR) \times 10^3$ | $p(RR) \times 10^3$ |
|---|---|---|---|---|---|---|---|---|---|
| KF100 | no | 0.442 | 0.0186 | 0.0184 | 0.0200 | $0.499_0$ | 3.8 | 40 | 1 |
| VP810 | no | 0.445 | 0.0175 | 0.0179 | 0.0194 | $0.498_8$ | 3.7 | 39 | 1 |
| S1010 | no | 0.440 | 0.0204 | 0.0196 | 0.0210 | 0.501 | 4.0 | 42 | 1 |
| D2000 | no | 0.425 | 0.0241 | 0.0242 | 0.0266 | $0.499_9$ | 5.1 | 54 | 8 |
| A5 | no | 0.437 | 0.0205 | 0.0204 | 0.0222 | $0.500_1$ | 4.2 | 45 | 7 |
| A6 | no | 0.432 | 0.0222 | 0.0217 | 0.0236 | $0.499_5$ | 4.5 | 47 | 6 |
| A7 | no | 0.436 | 0.0204 | 0.0207 | 0.0225 | $0.499_6$ | 4.3 | 45 | 5 |
| A8 | no | 0.436 | 0.0204 | 0.0206 | 0.0228 | $0.499_6$ | 4.3 | 46 | 2 |
| A9 | no | 0.437 | 0.0200 | 0.0203 | 0.0222 | $0.499_5$ | 4.2 | 44 | 2 |
| F1000 | 8 | 0.430 | 0.0230 | 0.0240 | 0.0260 | 0.503 | 5.0 | 52 | 22 |
| F50 | 13 | 0.424 | 0.0246 | 0.0240 | 0.0265 | $0.499_1$ | 5.0 | 54 | 19 |
| K460 | 44 | 0.409 | 0.0330 | 0.0280 | 0.0290 | $0.499_0$ | 5.7 | 61 | 53 |
| B1 | 35 | 0.403 | 0.0300 | 0.0300 | 0.0330 | 0.496 | 6.2 | 67 | 46 |
| B2 | 17 | 0.404 | 0.0320 | 0.0295 | 0.0327 | $0.499_2$ | 6.2 | 67 | 29 |
| B3 | 17 | 0.425 | 0.0245 | 0.0232 | 0.0265 | $0.499_2$ | 4.9 | 53 | 20 |
| B4 | <1 | 0.437 | 0.0202 | 0.0200 | 0.0224 | $0.499_6$ | 4.2 | 45 | 3 |
| B5 | 22 | 0.415 | 0.0277 | 0.0270 | 0.0300 | $0.499_7$ | 5.5 | 61 | 14 |

**Table 7** $^{19}F$ n.m.r. signals issued from the 20220 pentad. Approximate probabilities are computed with $p(F) \simeq p(FF) \simeq p(RF) = 1$

| Sequence | Sequence label | | Monomer sequences | Approximate probability |
|---|---|---|---|---|
| | Ref. 6 | Ref. 7 | | |
| 02020220020 | $D_1$ | $S^c_{211}$ | FFFRFF + RRFRRR | $p(FR) + p(R)p^3(RR)p(FR)$ |
| 02020220022 | $D_2$ | $S^c_{212}$ | FFFRFR + FRFRRR | $p^2(FR) + p^2(FR)p^2(RR)$ |
| 20020220020 | $D_3$ | $S^c_{221}$ | RFFRFF + RRFRRF | $p(R)p(FR) + p(R)p^2(RR)p(FR)$ |
| 20020220022 | $D_4$ | $S^c_{222}$ | RFFRFR + FRFRRF | $p(R)p^2(FR) + p^2(FR)p(RR)$ |
| 02020220200 | $D_5$ | $S^c_{112}$ | FFFRRF + RFFRRR | $p(FR)p(RR) + p(R)p(FR)p^2(RR)$ |
| 02020220202 | $D_6$ | $S^c_{111}$ | FFFRRR | $2p(FR)p^2(RR)$ |
| 20020220202 | $D_7$ | $S^c_{121}$ | RFFRRR + FFFRRF | $p(R)p(FR)p^2(RR) + p(FR)p(RR)$ |
| 20020220200 | $D_8$ | $S^c_{122}$ | RFFRRF | $2p(R)p(FR)p(RR)$ |

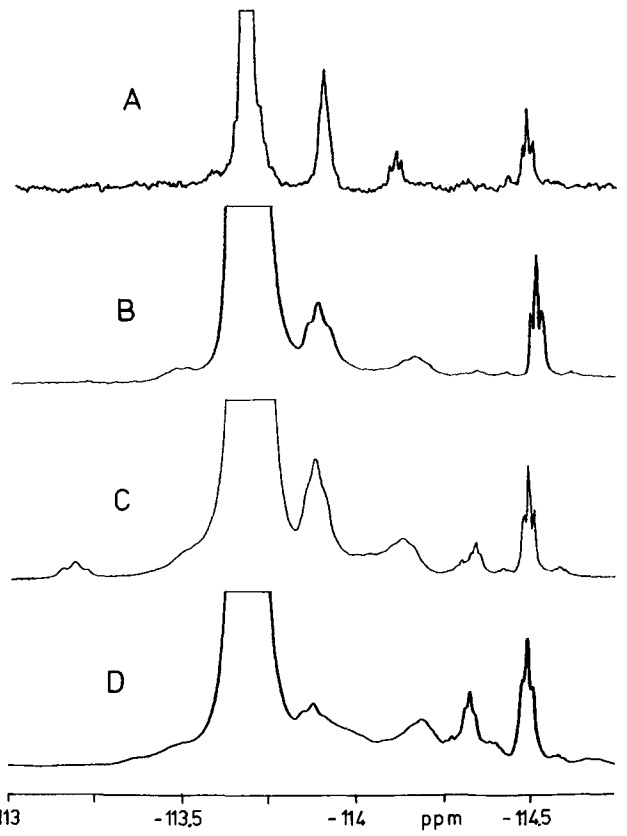


**Figure 6** Expansions of the C region (from −113 to −115 ppm) for comparison of two kinds of PVDF (same experimental conditions as *Figure 5*): (A) Solef 1010; (B) Daikin PVDF; (C) Foraflon 1000; (D) Kynar 460

soluble samples and $(0.7–3) \times 10^{-3}$ for microgel-forming samples.

It would be very interesting to identify directly in the group of lines C the signal corresponding to this sequence. The number of distinct signals recorded at 376 MHz suggests a resolution of sequences of 11 carbons, related to sequences of six monomers. These sequences have been enumerated by Ferguson and Ovenall[6] and Lovchikov *et al.*[7]. The eight lines derived from the pentad centred on a reversed addition 20220 are labelled D by the first authors and $S^c$ by Lovchikov. The sequences of carbons and the corresponding monomer sequences are given in *Table 7*. Since $p(F) \simeq p(FF) \simeq p(RF) \simeq 1$ their probabilities of occurrence can be product of small terms $p(R)$, $p(FR)$ and $p(RR)$ appearing in their expressions. It is clear that there should be one strong line ($D_1$ or $S^c_{211}$), four weaker lines ($D_2$, $D_3$, $D_5$ and $D_7$ or $S^c_{212}$, $S^c_{221}$, $S^c_{112}$ and $S^c_{121}$) and three hardly detectable lines in the C region. Moreover, for a first-order Markov process, $D_2 = D_3$ and $D_5 = D_7$. Among the four weak lines, two are sensitive to $p(RR)$. This is consistent with the spectra given by Ferguson[6] for one totally soluble (type I) PVDF (Kynar 961) and one partially soluble (type II) PVDF (Kynar 301) in DMAc. The former shows three weak lines, the latter five, but Ferguson and Ovenall retained only lines common to the two spectra, attributing the others to impurities. On the other hand, Lovchikov *et al.* published one spectrum in an unreferenced solvent where all eight lines are resolved and attributed, and their intensities claimed to fit a first-order Markov analysis.

Typical spectra of the C region are shown in *Figure 6* for two soluble and two 'gel-forming' samples in DMAc. Considering the narrow multiplet in all the spectra ($\delta = -114.5$ ppm, $J = 6$ Hz) as arising from an impurity, there seem to be only four detectable D lines. Among these, the line at −113.9 ppm strongly overlaps with the main $D_1$ or $S^c_{211}$ line at −113.7 ppm, making the determination of its intensity rather inaccurate. We have thus been unable to find a convincing correlation between calculated and observed intensities leading to unambiguous attribution of the weak lines. More work with different solvents and identification of impurities[12] is obviously needed to carry out a quantitative comparison of weak lines (level of $10^{-3}$ as compared to the total intensity) between 'soluble' and 'gel-forming' samples. This does not, however, invalidate the conclusions based on the analysis at the pentad level.

## CONCLUSIONS

Microgel-forming PVDF samples have been shown to be characterized not only by a slightly higher fraction of reversed head-to-head addition but also by a higher probability for not repairing a defect of reversed addition by an adjacent tail-to-tail addition. A formal identification by $^{19}F$ n.m.r. of the signal corresponding to the hypothetical $CF_2$-rich $-CH_2-CF_2-CH_2-CF_2-CF_2-CH_2-CF_2-CH_2-$, which is thought to be responsible for the formation of a physical microgel, has not been possible. One reason can be that their involvement in the microgel reduces their mobility and broadens their

signal. A correlation between a definite microstructure and the microgel-forming tendency is interesting from the points of view of both the optimization of the properties of PVDF and the general origin of physical gelation.

## ACKNOWLEDGEMENTS

Thanks are due to Mr A. Bieber (University Louis Pasteur, Strasbourg) for his help in setting a program for the calculations of the Markov parameters; to Mr Kappler (Atochem) for synthesizing the B samples; to Mr Breda (Atochem) for some of the s.e.c. results; to Mr Lecacheux (Elf-Aquitaine) for his help with s.e.c., and to Mr R. Graff (ICS) for his help in n.m.r. This work has benefited from a financial support of Atochem.

## REFERENCES

1 Lutringer, G. and Weill, G. *Polymer* 1991, **32**, 877
2 Lutringer, G., Meurer, B. and Weill, G. *Polym. Commun.* 1990, **31**, 235
3 Schwarzl, F. R. *Rheol. Acta* 1971, **10**, 166
4 Flory, P. J. 'Principles of Polymer Chemistry', Cornell University Press, Ithaca, NY, 1953
5 Lin Fu Tyan, Dissertation, University of Akron, 1979
6 Ferguson, R. C. and Ovenall, D. W. *Polym. Prepr., ACS Polym. Chem.* 1984, **25** (1), 340
7 Lovchikov, V. A., Shlyakov, A. M. and Dolgopolski, I. M. *Issled Stro. Makromol. Metodom Vysok.* 1983, 51–62 or ref. *Zh. Khim.* 1983, Abstr. **21**, 55
8 Cais, R. E. and Sloane, N. J. A. *Polymer* 1983, **24**, 179
9 Ferguson, R. C. and Brame, E. G. Jr *J. Phys. Chem.* 1979, **83**, 1397
10 Cais, R. E. and Kometani, J. M. *Macromolecules* 1985, **18**, 1357
11 Cais, R. E. and Kometani, J. M. *Macromolecules* 1984, **17**, 1887
12 Lutringer, G. and Weill, G. to be published